Diagnostics on electrically large structures by a nested skeletonization scheme enhancement of the equivalent current technique

L. Scialacqua[1], F. Mioc[1], L. J. Foged[1], G. Giordanengo[2], M. Righero[2], G. Vecchi[3]
[1] Microwave Vision Italy (MVI), Pomezia, Italy, (lucia.scialacqua, lars.foged)@microwavevision.com, francesca@mioc.info
[2] LINKS Foundation,Turin, Italy, (giorgio.giordanengo, marco.righero)@linksfoundation.com
[3] Antenna and EMC Lab, Politecnico di Torino, Italy, giuseppe.vecchi@polito.it

***Abstract*— The use of the Fast Multipole Method (FMM) in an equivalent current reconstruction technique, based on a dual-equation formulation, has been presented in the past for antenna design and diagnostics. The method was applied in design validation from measured data, demonstrating diagnostics feasibility of different large antennas up to an equivalent antenna volume of 2380 λ^3. Despite the computational advantages coming from the FMM, the memory request and the run time constraints could be still crucial in the processing of electrically large antennas. An enhancement of the equivalent current reconstruction technique based on a Nested Skeletonization Scheme is here presented. The new technique leads to a further reduction of memory requirements and computational time, applicable to diagnostic investigation of electrically larger problems in a wider frequency band. In this paper the nested skeletonization scheme enhancement of the equivalent current technique is applied and demonstrated for diagnostics on electrically large structures.**

***Index Terms*—Antenna measurements, antenna arrays, equivalent currents, fast methods, integral equations.**

I. INTRODUCTION

In recent 10-15 years diagnostics on electrically large structures is increasingly demanding due to more extensive applications at millimeter wave frequencies, especially in telecommunication, automotive and military areas.

The equivalent current reconstruction technique (EQC) see [1], [2] and also [3], [4] and[5]) has proved in the past to be an efficient method for antenna diagnostics and analysis, thanks to the FMM formulation, able to manage electrically large problems [6]. However, the continuous increase of dimensions of antenna problems requests the investigation of even larger problems, therefore a new technique based on a Nested Skeletonization Scheme (NSS) has been implemented. The new technique leads to a further reduction of memory requirements and computational time, allowing diagnostic investigation of electrically larger problems in a wider frequency band, without sacrificing accuracy. In particular, we show how the new technique efficiently handles fine meshes, which are often needed in cases where conformal surfaces are used to surround the antenna or where the EQC are used as input for a numerical simulation of the antenna mounted on a structure [7][8].

In this paper the diagnostic capabilities of this approach have been investigated on an electrically large radiator, consisting of a 32x8 linearly polarized array antenna (20λ x 6λ x 1λ @ 9.4 GHz). Comparison between the FMM technique, applied in the past on this antenna [6], and NSS method is carried out, to demonstrate the improvements in terms of computational time, allocated memory and accuracy of the results.

II. NESTED SKELETONIZATION SCHEME

The acceleration technique is based on a skeleton [9] representation of the source and test points. This is applied to both the enforcement of the null-field condition [1][2], in a way similar to a classical Method of Moment codes, and the matching of the measured data (see [1] and [10] for an example highlighting how the lack of the null-field condition hampers the diagnostic capabilities of the obtained currents).

Briefly, the method works as follow:

- The mesh where EQC live and the cloud of points where field data are acquired are both split with an octree.
- For each block at each level, we iteratively select a set of representative elements, i.e. the skeletons, and we build an interpolation matrix to interpolate a functions defined on the skeletons to a function defined on all the elements, and the corresponding anterpolation matrix. To select the skeletons and build the matrices, we use a proxy surface surrounding the box [9].
- Interactions between elements in octree boxes in the near field are computed directly, whereas interaction between elements in octree boxes which are not in near field are approximated using skeletons.

Once the interpolation and anterpolation matrices are build and the submatrices with the interactions between elements in the near field and between skeletons are populated, we can evaluate efficiently the matrix-vector product needed in the iterative solver used to solve the least-squares problems of source reconstruction [1][2].

We can select the skeletons and build the matrices working with proxy surfaces (with a number of degrees of freedom which can be set to control accuracy) and skeletons are built recursively from the finer levels to the highest [9], so the method scales favorably both in memory and in computational complexity with the number of unknowns.

III. LARGE 32X8 LINEARLY POLARIZED ARRAY ANTENNA

The antenna under test (AUT) is an X-band 32x8 patch array antenna, an array picture is shown in Fig. 1. The AUT has been designed to illuminate with a uniform distribution a target at the distance of 1m. AUT dimensions are LxWxH = 666 x 206 x 14mm (roughly 20 λ x 6 λ x 1λ, equivalent antenna volume equal to 120 λ^3). The array elements are very small compared to wavelength (less than λ/10), while the beam forming network (BFN), was realized to get a 15dB excitation taper in the vertical plane and an equal amplitude/phase distribution in the horizontal plane.

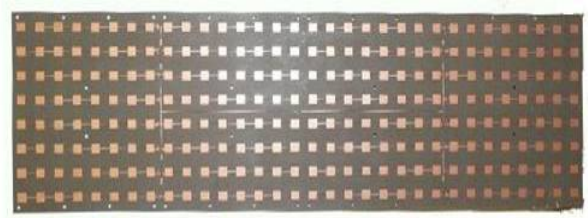

Fig. 1. AUT: Printed 32x8 patch array antenna.

The array has been measured in MVG StarLab (SL) multi-probe spherical Near Field NF system, see Fig. 2. Directivity radiation patterns @9.4GHz, on horizontal and vertical principal planes, are shown in Fig. 3. An asymmetry has been detected in the radiation pattern, especially on the horizontal plane, with respect to the predicted results from simulations. The EQC technique has been applied to the measured near field of the antenna to investigate the causes of this malfunctioning.

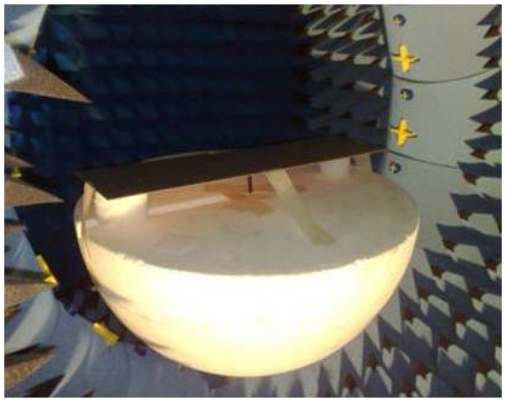

Fig. 2. Patch array during NF measurement within the MVG SL-18GHz measurement system.

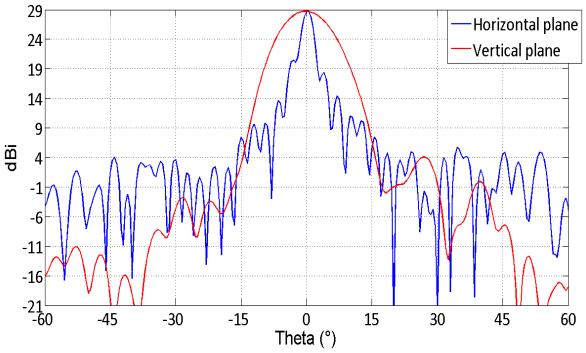

Fig. 3. Directivity radiation pattern of the array on the horizontal and vertical planes (prototype) @9.4GHz.

IV. RESULTS

The EQC technique, based on a dual-equation formulation [1], [2], has been applied to the AUT, using both the NSS and the FMM, with particular attention to allocated RAM, computational time, accuracy of the computed currents and accuracy of reconstructed Far Field.

A. Allocated RAM and computational time

In the past the FMM has been applied to this antenna for diagnostic with a mesh step of the computed domain of λ/4 @9.4GHz [6]. The investigation showed that the FMM was already able to manage acceptably such electrically large problem.

In this study we initially applied the NSS enhancement to the problem with the mesh step of λ/4 @9.4GHz. Moreover, we extended the same analysis on larger problems reducing the mesh step to λ/8, λ/16, up to λ/20 @9.4GHz. As briefly mentioned in Section I, meshes with edges smaller than λ/4 may be needed to follow a surface conformal to the AUT or to be compliant with request for other codes using the EQC, for example for simulations as in [7] and [8]. Even if the present case does not exhibit fine geometrical details requiring a mesh with small triangles, for the sake of comparison and validation, we stick to the example shown in [6], increasing the mesh resolution as a proxy for more complex cases. The measured NF consists of 11200 data samples.

The dimensions of the problem, in terms of number of basis functions and numerical system size for the different mesh steps, are reported in Table I. The system size is the product between the number of measured sample points (real and imaginary part values) and the number of basis functions (for J and M currents correspondent to the edges of the triangles of the mesh). This represents the dimensions of the linear problem to be inverted by the equivalent current method.

TABLE I. TEST CASES OF DIFFERENT ELECTRICAL DIMENSIONS, INVESTIGATED BY THE FMM AND NSS TECHNIQUES.

Mesh step	N functions (mesh)	System size [10^9]
λ/4	39840	8.92495680
λ/8	149424	33.47396448
λ/16	619872	138.86372544
λ/20	972720	217.90873440

The allocated RAM and computational time have been evaluated for all the selected test cases and complete results are reported in Fig. 4 and Fig. 5, respectively. In both plots the blue dots are the value for the FMM technique and the orange dots for the NSS technique.

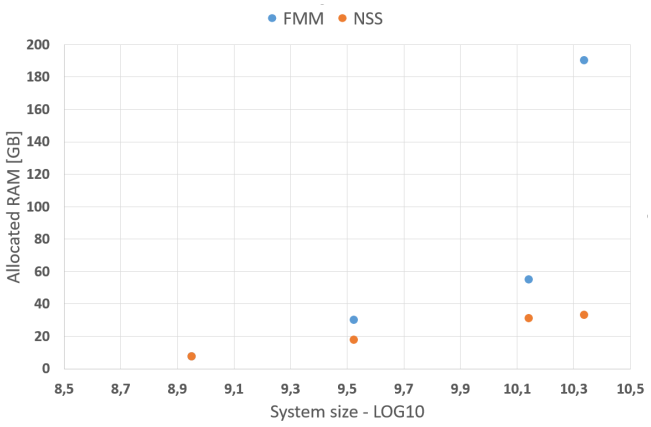

Fig. 4. Allocated RAM (GB) vs system size. The computations have been performed by the FMM and the NSS techinques.

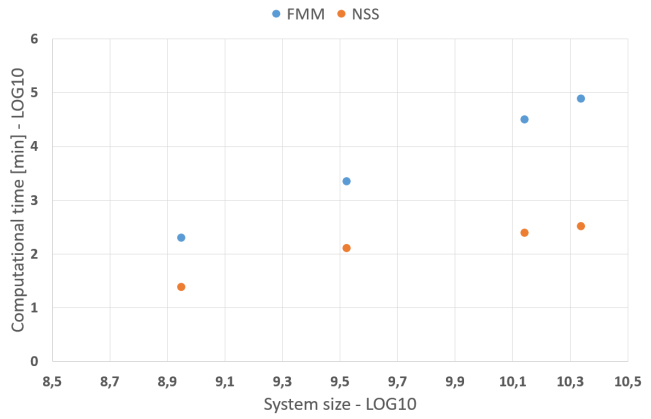

Fig. 5. Computational time (minutes) vs system size. The computations have been performed by the FMM and the NSS etechinques .

It is interesting to observe for this test case that for a mesh at λ/4 the allocated RAM using the NSS enhancement is almost the same of FMM, instead the computational time is reduced respect to FMM. The percentage reduction of the computational time is 8.3. Conversely when the electrical dimensions of the problem (system size) are increased for NSS there is a reduction of computational time and RAM respect to FMM. The percentage reduction increases as the problem dimensions increase.

The percentage reduction for computational time and RAM of NSS versus FMM are summarized in Table II.

TABLE II. PERCENTAGE REDUCTION OF THE COMPUTATIONAL TIME AND RAM, USING NSS VS FMM TECHNIQUE.

	Percentage Reduction NSS vs FMM	
Mesh step	Computational time %	RAM %
λ/4	87.9	0.0
λ/8	94.3	41.3
λ/16	99.2	43.6
λ/20	99.6	72.5

B. Reconctructed equivalent currents and accuracy of the reconstructed Far Field pattern

The amplitude of the reconstructed electric currents (J) on the upper face of the reconstruction surface with co-polar and cross-polar components, respectively, are shown in Fig. 6. The current distribution on the array is corresponding to the one evaluated in the past with FMM [1] confirming the same diagnostic conclusions. Indeed, also the results from NSS method highlights that part of the asymmetry on the pattern is associated to the miscalculation of the electrical length of the BFN feeding lines, then no constant phase excitation occurs in the horizontal plane.

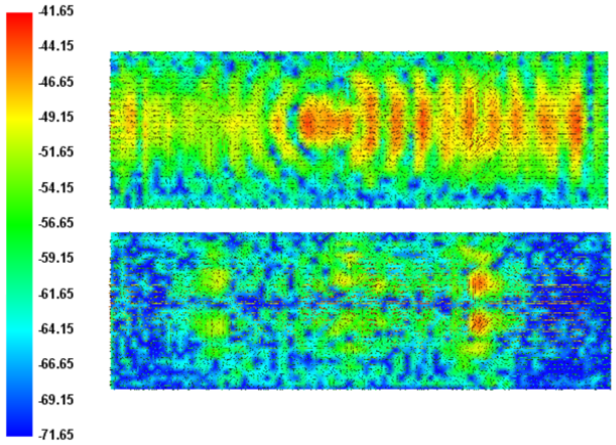

Fig. 6. Reconstructed equivalent J by the technique based on a NSS, co-polar currents [dB] (upper figure) and cross-polar currents [dB] (lower figure).

In order to quantify the accuracy of the results computed by the new technique the Equivalent Noise Level (ENL) defined as,

$$ENL = 20\log_{10}\left(RMSE\left|\frac{E(\theta,\varphi) - \tilde{E}(\theta,\varphi)}{E(\theta,\varphi)_{MAX}}\right|\right)$$

is considered. In such expression $E(\theta,\varphi)$ is the reference and $\tilde{E}(\theta,\varphi)$ is the pattern under analysis.

The input measured field has been considered as reference field, while the pattern reconstructed from the computed equivalent current is the one under analysis. The ENL has been evaluated on the whole pattern considering the total field. The obtained ENL is reported in Table III for the for the FMM and NSS enhancement.

TABLE III. ENL ON THE WHOLE PATTERNS.

FMM [dB]	NSS [dB]
-48.8426	-50.2471

The accuracy of both methods FMM and NSS is of the same order.

V. CONCLUSION

The nested skeletonization scheme enhancement of the equivalent current technique is applied and demonstrated for diagnostics on electrically large structures. The study has been carried out on an electrically large radiator, consisting of large a 32x8 linearly polarized array antenna (20λ x 6λ x 1λ @ 9.4 GHz). Comparison between the Fast Multipole Method (FMM), applied in the past on this antenna [6] and NSS has been carried out, to demonstrate the improvements in terms of computational time, allocated memory and accuracy of the results.

In this test case, for a mesh with triangular step of λ/4 @9.4GHz, the detected allocated RAM is almost the same, instead it exhibits a relevant reduction of computational time of a factor 8.3. For larger electrical problems (up to a mesh step of λ/20 @9.4GHz) improvements are impressive. Computational time is reduced by 99.6%, while RAM is lowered of 72.5%.

Tests on the complexity scaling as a function of the electrical dimension of the AUT are the subjects of current investigation. Analysis of the currents by the nested skeletonization scheme enhancement confirms accurate results respect to the one computed in the past with the FMM [1], confirming the validity of the diagnostic investigation.

For better evaluation on accuracy of the results, the Equivalent Noise Level (ENL) on the Far Field radiation patterns before (measured input) and after the equivalent current reconstruction have been analyzed for NSS and FMM. The accuracy of both methods FMM and NSS are comparable with a small improvement due to the new technique.

REFERENCES

[1] J. A. Quijano and G.Vecchi, "Field and source equivalence in source reconstruction on 3D surfaces," Prog. Electromagn. Res., no. PIER 103, pp. 67–100, 2010.

[2] J. Araque and G. Vecchi, "Improved-accuracy source reconstruction on arbitrary 3-D surfaces," IEEE Antennas Wireless Propag. Lett., vol. 8, pp. 1046–1049, 2009.

[3] K. Persson, M. Gustafsson, and G. Kristensson, "Reconstruction and visualization of equivalent currents on a radome using an integral representation formulation," Progress In Electromagnetics Research B, vol. 20, pp. 65–90, 2010.

[4] T. F. Eibert and C. H. Schmidt, "Multilevel fast multipole accelerated inverse equivalent current method employing Rao-Wilton-Glisson discretization of electric and magnetic surface currents," Antennas and Propagation, IEEE Transactions on,vol. 57, no. 4, pp. 1178–1185, April 2009.

[5] Y. Alvarez, F. Las-Heras, and M. Pino, "Reconstruction of equivalent currents distribution over arbitrary three-dimensional surfaces based on integral equation algorithms," Antennas and Propagation, IEEE Transactions on, vol. 55, no. 12, pp. 3460–3468, Dec. 2007.

[6] L.J. Foged, L. Scialacqua, F. Saccardi, J. L. Araque Quijano, G. Vecchi, "Application of the Dual-Equation Equivalent Current Reconstruction to Electrically Large Structures by Fast Multipole Method Enhancement", 35th Annual Meeting and Symposium - Antenna Measurement Techniques Association, AMTA 2013, October 2013, Columbus, Ohio, USA.

[7] L. J. Foged et al., "Bringing numerical simulation and antenna measurements together," The 8th European Conference on Antennas and Propagation (EuCAP 2014), The Hague, 2014, pp. 3421-3425. doi:10.1109/EuCAP.2014.6902564

[8] L. J. Foged et al., "Innovative representation of antenna measured sources for numerical simulations," 2014 IEEE Antennas and Propagation Society International Symposium (APSURSI), Memphis, TN, 2014, pp. 2014-2015. doi: 10.1109/APS.2014.6905334

[9] M. A. E. Bautista, M. A. Francavilla, P. Martinsson and F. Vipiana, "$\mathcal {O}(N)$ Nested Skeletonization Scheme for the Analysis of Multiscale Structures Using the Method of Moments," in IEEE Journal on Multiscale and Multiphysics Computational Techniques, vol. 1, pp. 139-150, 2016. doi: 10.1109/JMMCT.2016.2645838

[10] M. S. Castaner, L. J Foged (eds.), "Post-processing Techniques in Antenna Measurement", Institution of Engineering and Technology (Electromagnetic Waves series), 2019

[11] J. L. Araque Quijano, L. Scialacqua, J. Zackrisson, L. J. Foged, M. Sabbadini, G. Vecchi "Suppression of undesired radiated fields based on equivalent currents reconstruction from measured data", Antennas Wireless Propag. Lett., vol. 10, 2011 p314-317.

[12] Insight software website: https://www.mvg-world.com/en/products/field_product_family/antenna-measurement-2/insight